Anal Bioanal Chem
DOI 10.1007/s00216-017-0355-1

RESEARCH PAPER

Functional gold nanoparticles for optical affinity biosensing

Tomáš Špringer[1] · **Xue Chadtová Song**[1] · **Maria Laura Ermini**[1] · **Josefína Lamačová**[1] · **Jiří Homola**[1]

Received: 6 January 2017 / Revised: 16 March 2017 / Accepted: 31 March 2017

Abstract Functional gold nanoparticles (AuNPs) are commonly used to enhance the response of optical affinity biosensors. In this work, we investigated the effect of preparation conditions on functional properties of AuNPs functionalized with antibody (Ab-AuNPs), specifically AuNPs with antibody against carcinoembryonic antigen (CEA) covalently attached via carboxy-terminated oligo-ethylene thiolate linker layer. The following parameters of preparation of Ab-AuNP have been found to have a significant effect on Ab-AuNP performance in affinity biosensors: the time of reaction of activated AuNPs with antibody, concentrations of antibody and amino-coupling reagents, and composition of immobilization buffer (molarity and salt content). In contrast, pH of immobilization buffer has been demonstrated to have only a minor influence. Our experiments showed that the Ab-AuNPs prepared under optimum conditions offered a binding efficiency of Ab-AuNPs to CEA as high as 63%, which is more than 4 times better than the best efficiencies reported for similar functional AuNPs so far. We employed these Ab-AuNPs with a surface plasmon resonance (SPR) biosensor for the detection of CEA and showed that the Ab-AuNPs enhanced the sensor response to CEA by a factor of 1000. We also demonstrated that the Ab-AuNPs allow the biosensor to detect CEA at concentrations as low as 12 and 40 pg/mL in buffer and 50% blood plasma, respectively.

Keywords Functionalization · Gold nanoparticles · Antibody · Optical affinity biosensor · Surface plasmon resonance · Cancer marker carcinoembryonic antigen

Introduction

Functional gold nanoparticles (AuNPs) are widely used in optical affinity biosensors to enable detection of low concentrations of biologically relevant molecules [1, 2]. The limit of detection (LOD), one of the most important biosensor performance characteristics [3], is in a large part determined by the performance of functional AuNPs, in particular, by the efficiency of the binding of functional AuNPs to target molecules (specific binding) and the level of binding of AuNPs to non-target molecules (nonspecific binding) [1]. The specific and nonspecific binding of AuNPs therein influences the enhancement of the sensor response to the target analyte and the variability of the sensor response in control experiments, respectively.

In recent years, various functional AuNPs have been reported. These include AuNPs functionalized with (i) oligonucleotide probes [4–6], (ii) mixture of oligonucleotide probes and antibodies [7], and (iii) proteins [8]. The performance of functional AuNPs in affinity biosensors strongly depends on the chemistry used to attach biorecognition elements (receptors) to AuNP surface [9, 10]. In the overwhelming majority of biosensor studies, protein receptors have been adsorbed onto the surface of AuNPs. For instance, this approach has been previously applied in the preparation of functional AuNPs for the detection of cancer markers including prostate-specific antigen (PSA) and carcinoembryonic antigen

Electronic supplementary material The online version of this article (doi:10.1007/s00216-017-0355-1) contains supplementary material, which is available to authorized users.

✉ Tomáš Špringer
springer@ufe.cz

✉ Jiří Homola
homola@ufe.cz

[1] Institute of Photonics and Electronics, Czech Academy of Sciences, Chaberská 57, Prague, Czech Republic

Published online: 17 April 2017

(CEA) [8, 11–15]. As the functional AuNPs prepared using this approach often suffer from both high nonspecific binding and low stability [9, 10], several authors have thus advocated the covalent attachment of receptors to AuNPs via a linker layer [9, 10]. However, this approach has been rarely studied [16, 17].

The immobilization of molecular receptors onto a surface of AuNP via a linker layer is a delicate process and is very sensitive to the conditions under which immobilization is performed; however, little is known about the role of the conditions in the immobilization process. To our knowledge, the only discussion on the topic is the work from Bartczak and Karanas, who investigated the effect of different preparation conditions on the immobilization efficiency of a short 8-mer peptide onto AuNPs coated with carboxy-terminated oligo-ethylene glycol (OEG) thiolates [18]. Nevertheless, the work did not investigate the effect of the preparation conditions on the performance of the developed AuNPs in optical affinity biosensors and, thus, cannot serve as a guide for the preparation of functional AuNPs for optical affinity biosensors.

In this work, we investigated the effect of preparation conditions on the functional properties of AuNPs functionalized with antibody (Ab-AuNPs), specifically AuNPs with antibody against CEA covalently attached via carboxy-terminated oligo-ethylene thiolate linker layer. We investigated the effect of (a) the reaction time of the activated AuNPs with antibodies, (b) the concentrations of antibody and amino-coupling reagents, and (c) the composition of the immobilization buffer. We quantified the performance of the prepared Ab-AuNPs in terms of both specific and nonspecific binding using a surface plasmon resonance (SPR) biosensor and a sandwich assay for the detection of CEA in which Ab-AuNPs are binding to CEA molecules previously captured by antibodies immobilized on the SPR biosensor surface. We further applied the Ab-AuNPs prepared under optimum conditions in the sensitive detection of CEA.

Materials and methods

Reagents

Sodium acetate, KH_2PO_4, Na_2HPO_4, KCl, NaCl, NaOH, ethanolamine (EA), 3-(*N*-morpholino)propanesulfonic acid (MOPS), $HAuCl_4{\cdot}3H_2O$ (99%), trisodium citrate (99%), and bovine serum albumin (BSA) were purchased from Sigma-Aldrich, USA, in molecular biology grade or higher. *N*-hydroxysuccinimide (NHS) and 1-ethyl-3-(3-dimethylaminopropyl)-carbodiimide hydrochloride (EDC) were purchased from GE Healthcare, USA. CEA (200 kDa) and monoclonal primary antibody against CEA (Ab_1) and monoclonal secondary antibody against CEA (Ab) were purchased from Fitzgerald, USA. Antibody against *Salmonella* (Ab_R) was obtained from KPL, Inc., USA. Carboxy-[HS-C_{11}-$(EG)_6$-OCH_2-COOH] (HS-OEG-COOH), hydroxy-[HS-C_{11}-$(EG)_4$-OH] (HS-OEG-OH), and amino-terminated HS-C_{11}-$(EG)_6$-NH_2 oligo-ethylene glycol thiols were purchased from Prochimia, Poland. Ethanol for spectroscopy (purity 99.9% or greater) was purchased from Merck, USA.

The composition of phosphate buffer was 1.4 mM KH_2PO_4, 8 mM Na_2HPO_4, and 2.7 mM KCl, pH 7.4. PBS and PBS_{NaCl} consisted of phosphate buffer with the addition of 137 and 750 mM NaCl, respectively. PBS_{BSA} buffer was prepared by adding 250 μg/mL BSA into PBS. SA_{10} consisted of 10 mM sodium acetate, pH 5. Phosphate buffer at 0.5 mM (PB) consisted of 0.1 mM KH_2PO_4 and 0.4 mM Na_2HPO_4, pH 8. Phosphate buffer at 5 mM (PBS_0) consisted of 1 mM KH_2PO_4 and 4 mM Na_2HPO_4, pH 7.4. During the functionalization of AuNPs, immobilization MOPS buffers (molarity, pH, and concentration of NaCl are described in the text) were used. All buffers were prepared using deionized water (Q-water, 18 MΩ/cm resistivity, Direct-Q UV3, Millipore, USA). Spherical AuNPs with a diameter of (40 ± 5) nm (measured with a scanning electron microscope (SEM) e_LiNE Plus, Raith, Germany) were prepared by the reduction of $HAuCl_4$ with sodium citrate [19].

Normal human plasma (mixed/pooled gender) in sodium citrate was purchased from Biochemed Services. Fifty percent plasma was prepared by mixing the undiluted (100%) human plasma and PBS with 10 mg/mL BSA in a ratio of 1:1.

Preparation of Ab-AuNPs

AuNPs were modified with carboxy-terminated thiols activated with amino-coupling reagents and coated with Ab (see Fig. 1a). The preparation of Ab-AuNPs is described below. For the functionalization of AuNPs with carboxy-terminated thiols, we centrifuged AuNPs (9500*g* for 10 min in Universal 320R, Hettich Zentrifugen, Germany), the supernatant was removed, and AuNPs were dissolved in PB to the AuNP concentration of 0.33 nM. Then, HS-OEG-COOH at a concentration of 333 μM was added into the solution of washed AuNPs. This mixture was sonicated in a water bath (50 °C) for 1 h and shaken overnight at room temperature. The unreacted HS-OEG-COOH was then removed from the solution using repeated washing cycles: the solution with thiolated AuNPs was centrifuged (9500*g*, 10 min), the supernatant was removed, and the thiolated AuNPs were dissolved in Q-water. To covalently attach Ab, 250 μL of thiolated AuNPs at a concentration of 0.275 nM was mixed with 25 μL NHS/EDC solution (total concentration of NHS/EDC, c_{total} = 0.003, 0.03, 0.3, 0.9, 3, 6, and 15 mM, ratio NHS:EDC = 1:5) for 5 min. This mixture was centrifuged at 9500*g* for 3 min, and the supernatant was removed. The activated thiolated AuNPs were dissolved in 250 μL immobilization MOPS buffer with Ab (c = 0, 3, 6, 9, 12, 15, 18, 21, 24, 30, 90, 150 μg/mL), and the solution was shaken for 0.5, 1, 3, 6, or 12 h (reaction time).

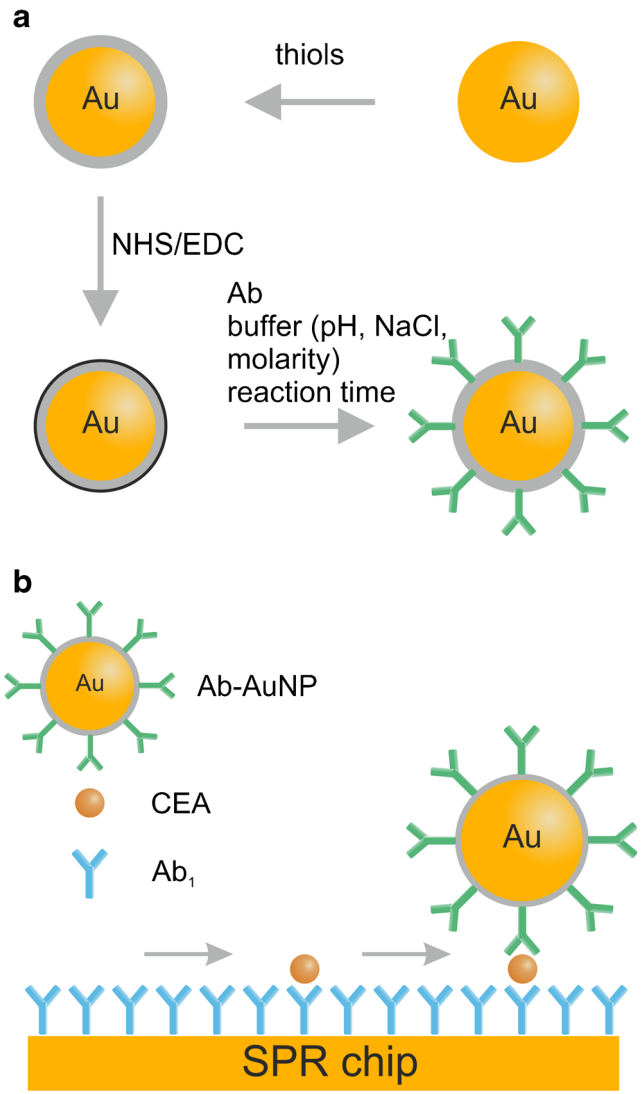

Fig. 1 **a** Scheme of Ab-AuNP preparation. **b** Sandwich assay used in the SPR experiments

The following parameters of the immobilization buffer (MOPS) were varied: (i) pH (6.5, 7, 7.4, 7.9, 8.4, and 8.9), (ii) the amount of added NaCl (0, 0.1, 0.3, 1, 3, 10, 30, and 100 mM), and (iii) molarity (0.5, 1, 3, 10, 30, and 100 mM). It is worth noting that MOPS also contained sodium cations that were added during the adjustment of pH (see Electronic supplementary material (ESM)). Then, 10 μL of 1 M EA was added into the solution with Ab-AuNPs, and this mixture was incubated for 5 min in order to deactivate all of the nonreacted esters. Unbound Ab was removed from the solution in repeated washing cycles (9500*g*, 10 min, Q-water). The solution of Ab-AuNPs was stored in a refrigerator until use. Prior to SPR measurement, the solution with Ab-AuNPs was centrifuged (9500*g* for 10 min) and the pellet was dissolved in PBS_{BSA}. The molar concentrations of AuNPs and Ab-AuNPs were determined according to the theory published in ref. [20].

In order to confirm that the used preparation method yields individual (unaggregated) Ab-AuNPs, we measured and analyzed the absorption spectra of Ab-AuNPs using an absorption spectrophotometer (NanoPhotometer Pearl UV-Vis, Implen, Germany). In addition, Ab-AuNPs prepared under the optimum conditions were captured on the surface of an SPR chip and were inspected using SEM (e_LiNE Plus, Raith, Germany). The samples for SEM were prepared as follows. A bare SPR chip was rinsed with Q-water and ethanol, cleaned in an ozone cleaner for 10 min, and rinsed with Q-water and ethanol. Then, the chip was mounted into the SPR biosensor and PBS was injected. Thiol $HS\text{-}C_{11}\text{-}(EG)_6\text{-}NH_2$ diluted in PBS with the final concentration of 80 μg/mL was injected for 10 min to bind to the surface of the SPR chip. Then, Ab-AuNPs (concentration 0.033 nM) were allowed to flow along the sensor surface until the sensor response of 6 nm was achieved. Then, the surface was flushed with PBS and Q-water. Finally, the chip was removed from the SPR biosensor and dried with a stream of nitrogen. SEM images showed that individual Ab-AuNPs were distributed across the surface of the chip confirming that the optimum procedure produces unaggregated or noncross-linked Ab-AuNPs (see ESM). To investigate the stability of Ab-AuNPs (prepared under optimum conditions) in PBS_0 with the addition of 140, 300, 500, 750, and 1000 mM NaCl, 0.15 nM Ab-AuNPs were incubated for 3 h in these solutions and the absorption spectra of the solutions were measured. The experiments confirmed that the Ab-AuNPs used in the model detection assay were stable in all these solutions for at least 3 h.

SPR biosensor

In this study, we used a laboratory SPR platform based on the wavelength spectroscopy of surface plasmons (plasmon IV) [21] with dispersionless microfluidics [22, 23]. In this type of SPR sensor, the angle of incidence of the light beam is fixed and the SPR dip is observed in the spectrum of polychromatic light coupled to a surface plasmon. The sensor response is expressed in terms of the shift in the wavelength at which the SPR dip occurs. This response is sensitive to changes in the refractive index caused by the binding of molecules to the surface of an SPR chip. A shift of 1 nm in the SPR wavelength represents a change in the protein surface coverage of 17 ng/cm^2 [17]. SPR chips used in this work were prepared by coating BK7 glass substrates with thin layers of titanium (1–2 nm) and gold (48 nm) via e-beam evaporation in vacuum. The SPR chips were functionalized with a self-assembled monolayer (SAM) of mixed carboxy-terminated and hydroxy-terminated OEG thiols, on which primary antibody Ab_1 (for the characterization of Ab-

AuNPs functionalized under different conditions) or Ab_1 and BSA (for the detection of CEA with Ab-AuNPs prepared under optimum conditions) were immobilized using the amino-coupling as described previously [17]. Initially, a 3:7 molar mixture of HS-OEG-COOH and HS-OEG-OH thiols was dissolved in ethanol at a total concentration of 0.2 M. A clean SPR chip was immersed in the thiol mixture for 10 min at 40 °C and stored at room temperature for at least 12 h. Then, the chip was rinsed with ethanol and Q-water and mounted into the SPR sensor. SA_{10} buffer was pumped along the SPR chip surface for 5 min, after which the chip surface was incubated in a mixture of 12.5 mM NHS and 62.5 mM EDC (dissolved in SA_{10}) for 10 min to activate the carboxylic groups. After activation, primary antibody Ab_1 or antibody Ab_R at a concentration of 10 μg/mL in SA_{10} was injected for 15 min to covalently attach antibodies to the activated carboxylic groups. In the experiments, in which the Ab-AuNPs prepared under optimum conditions were used to detect CEA, 1 mg/mL BSA was further injected for 15 min. Then, the short injection of SA_{10} and PBS_{NaCl} was performed to remove the noncovalently bound molecules. After another short injection of SA_{10}, 1 mM aqueous EA (pH 8 at 25 °C) was pumped along the surface for 5 min to deactivate the remaining carboxyl groups. During the experiments reported in this paper, flow rate and temperature were kept at 20 μL/min and 25 °C, respectively.

Effect of preparation conditions on the performance of Ab-AuNPs

In order to characterize the influence of preparation conditions on the performance of Ab-AuNPs in optical biosensors, we employed Ab-AuNPs prepared under different conditions in the sandwich assay (Fig. 1b). As the number of combination of the above-listed parameters is large and beyond the scope of a single study, in our experiments, we always varied only a single parameter, while other parameters were kept constant. We used two channels of the SPR biosensor (both functionalized with Ab_1) to measure the specific and nonspecific binding of Ab-AuNPs. In the first channel, we flowed PBS_{BSA} for at least 15 min, then injected 500 ng/mL (2.5 nM) CEA in PBS_{BSA} for several minutes to achieve the sensor response of 0.15 nm (corresponds to the surface coverage of 8×10^9 CEA/cm^2 ~ about 10% of the maximum surface coverage). After a short injection of PBS_{BSA}, we injected a solution containing Ab-AuNPs at a concentration of 0.033 nM for 1 min. The PBS_{BSA}/Ab-AuNPs cycle was repeated with Ab-AuNPs prepared under different conditions. Measurement in the second channel followed the same protocol with two modifications:(i) no CEA was injected and (ii) a solution containing Ab-AuNPs was injected for 4 min (to obtain a sufficiently large sensor response). The sensor response to the nonspecific binding of Ab-AuNPs was determined as a slope of the Ab-AuNP binding curve in the second channel. The sensor response to the specific binding of Ab-AuNPs was determined as a difference between the slopes of the Ab-AuNP binding curves in the first and second channels. To confirm that the partial coverage of the surface of the SPR chip with previously captured Ab-AuNPs does not influence the response of the sensor to the Ab-AuNPs used in later cycles, we run a batch of reference Ab-AuNPs before the first and after the last batch of tested Ab-AuNPs and compared the sensor responses. Sensor response to each type of Ab-AuNPs was measured at least three times on at least three different chips.

Detection of CEA with the developed Ab-AuNPs

In order to evaluate the performance of the Ab-AuNPs prepared under optimum conditions, we used these Ab-AuNPs in the sandwich assay to detect CEA in PBS_{BSA} and in 50% plasma (see Fig. 1b). For the detection of CEA diluted in PBS_{BSA} (=buffer), we used the detection and reference channels functionalized with Ab_1 and Ab_R, respectively. For the detection of CEA in 50% plasma (=plasma), both detection and reference channels were functionalized with Ab_1. The step-by-step description of the detection protocol is provided below.

(1) For buffer and plasma: The sensor surface in both the detection and reference channels was incubated in PBS_{BSA} for at least 15 min. (2) For buffer: CEA at concentrations of 0.0625, 0.125, 0.25, 0.75, 2.5, 12.5, 25, 50, 125, 250, 625, 1250, and 2500 ng/mL was injected for 20 min into both detection and reference channels. For plasma: 50% plasma either without added CEA (reference channel) or spiked with 0.0625, 0.125, 0.5625, 2.5, 25, 50, 125, 250, 625, and 1250 ng/mL CEA (detection channel) was injected for 20 min. (3) For buffer: PBS_{BSA} was injected for several minutes into both channels and the direct sensor response to CEA was determined. For plasma: PBS_{BSA}, PBS_{NaCl} (3 min), and PBS_{BSA} were injected for several minutes into both detection and reference channels to decrease the amount of plasma components adsorbed on the surface of the SPR chip, and the direct sensor response to CEA was determined. (4) For buffer and plasma: Ab-AuNPs (concentration 0.77 nM) prepared under optimum conditions were injected for 25 min. After short injection of PBS_{BSA}, the Ab-AuNP-enhanced response was determined for CEA concentrations below 250 ng/mL. Because the plasma sample naturally contains low levels of CEA [2] (~1.5 ng/mL CEA for our 50% plasma), we used the referencing method developed previously in our laboratory [17, 24] to determine the nonspecific binding of Ab-AuNPs to the surface of the SPR chip. This was implemented by adding 5 μg/mL Ab_1 into 50% plasma in step (2) of the detection experiment.

The specific sensor response to both CEA and Ab-AuNPs was calculated by subtracting the sensor response in the reference channel from that in the detection channel. Each detection experiment was repeated at least three times, each time on a different chip. The binding efficiency of Ab-AuNPs to CEA was determined as a ratio of the surface density of specifically bound Ab-AuNPs (see our previous work [16]) and the surface density of CEA (see our previous work [17]). LOD was calculated as the concentration that corresponds to twice the critical level of the sensor response, which is related to that from a blank sample (Student's *t* test, 12 replicates, significance level of 5%).

Results and discussion

In the following sections, we present the results of the investigation of the effects of various preparation conditions on the performance of Ab-AuNPs. Therein, we use the figure of merit *R* defined as a ratio of specific sensor response (SSR) of Ab-AuNPs and the nonspecific sensor response (NSR) of Ab-AuNPs in order to compare the performance of different types of Ab-AuNPs. In the last section, we report on the results of model CEA detection experiments in which Ab-AuNPs prepared under optimum conditions were employed.

Effect of concentration of Ab

Figure 2 shows SSR, NSR, and *R* for Ab-AuNPs prepared using different concentrations of Ab in immobilization buffer. As depicted in Fig. 2, SSR asymptotically increased with Ab concentration, which was most likely associated with an increase of Ab surface density on AuNPs. No decrease of SSR was observed at higher Ab concentrations, suggesting that there were no effects of overcrowding at higher Ab concentrations [25]. In contrast, the effect of Ab concentration on the NSR was more complex with a minimum NSR value at Ab concentration of about 9 μg/mL. This behavior can likely be attributed to two different mechanisms, each of which takes dominance at low and high Ab surface densities. We believe that the initial decrease in NSR (at low Ab concentrations) was due to a decrease in electrostatic interactions between the positive partial charges on Ab_1 (on the surface of a chip) and the negatively charged carboxylic groups on the AuNPs (which decreased with increasing Ab concentrations) [26]. At higher Ab concentrations, this effect became mitigated, and the increase of NSR might be caused by the increase of the intermolecular attractions between Ab_1 bound to the sensor surface and the (increasing) Ab density on AuNPs [27]. The maximum value of *R* was achieved for a relatively narrow range of Ab concentrations (from 9 to 30 μg/mL).

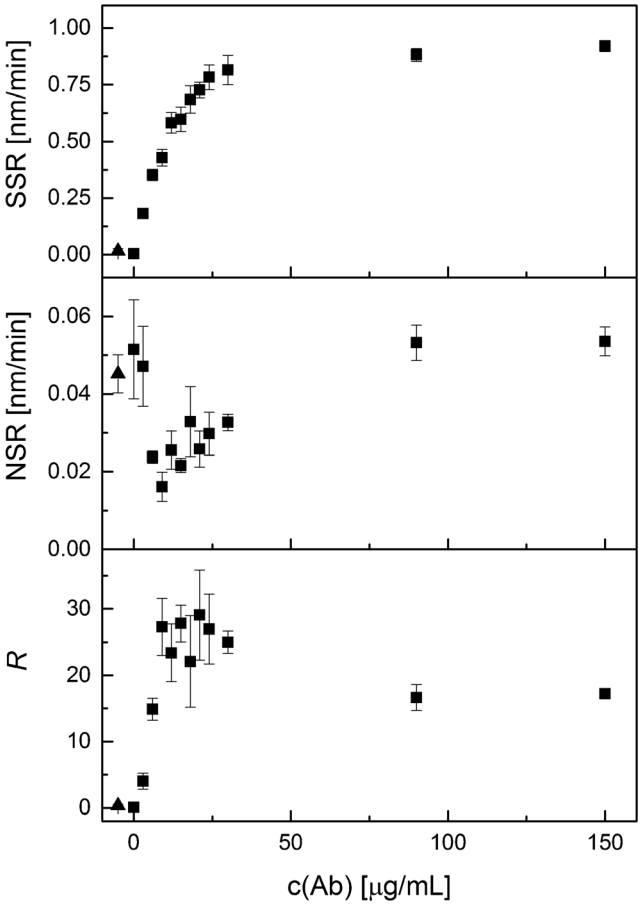

Fig. 2 SSR, NSR, and *R* for Ab-AuNPs prepared with different concentrations of Ab in immobilization buffer (*squares*). Preparation conditions kept constant: 3 mM NHS/EDC, 3 h reaction time, 1 mM MOPS with 0 mM NaCl and pH 7.4. SSR, NSR, and *R* were also determined for thiolated AuNPs (*triangles*)

Effect of concentration of NHS/EDC

SSR of Ab-AuNPs was found to increase rapidly with the concentration of NHS/EDC in solution until the NHS/EDC concentration of 3 mM and then started to decrease (Fig. 3). We think that this behavior was a result of the interplay between the density of Ab that increased with the concentration of NHS/EDC and the flexibility of the immobilized Ab that decreased with the increasing concentration of NHS/EDC due to the antibody attachment through multiple amino groups. The argument of reduced flexibility was supported by the control experiments which we performed with Ab immobilized on a flat surface of the SPR chip (see ESM). NSR was observed to depend on the concentration of NHS/EDC only weakly. The mild decrease of NSR at higher NHS/EDC concentrations may be in part associated with the increasing amount of antibody attached to the surface of AuNPs. As depicted in Fig. 3, *R* exhibited high values for a

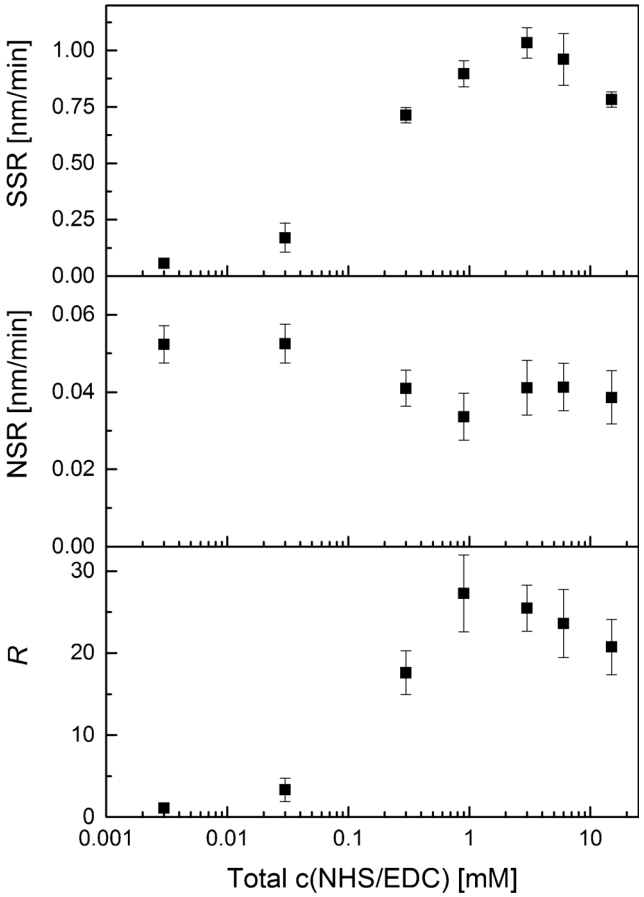

Fig. 3 SSR, NSR, and *R* for Ab-AuNPs prepared using different concentrations of NHS/EDC. Preparation conditions kept constant: 30 μg/mL Ab, 3 h reaction time, 1 mM MOPS with 0 mM NaCl and pH 7.4

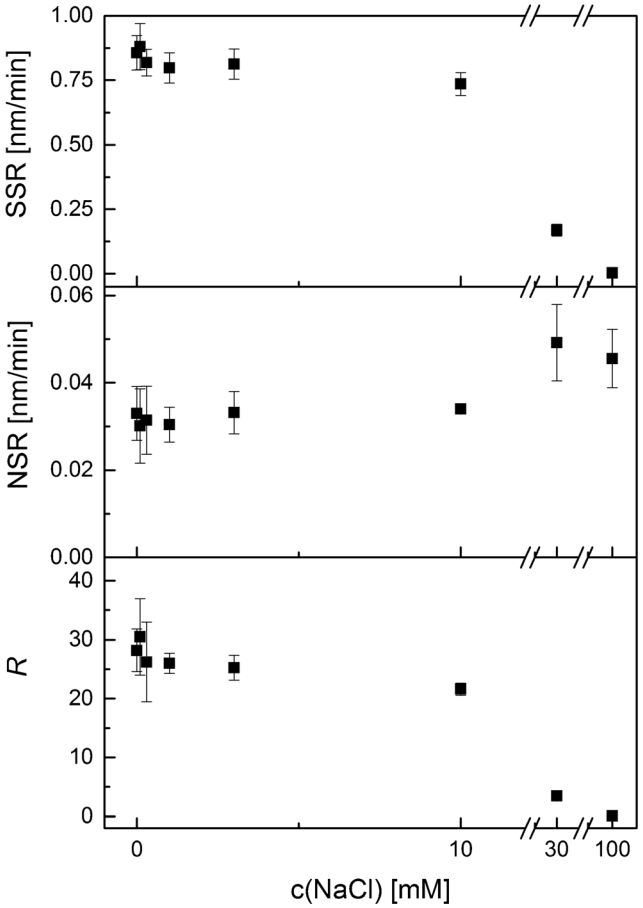

Fig. 4 SSR, NSR, and *R* for Ab-AuNPs prepared with the different concentrations of NaCl in immobilization buffer. Preparation conditions kept constant: 3 mM NHS/EDC, 30 μg/mL Ab, 3 h reaction time, 1 mM MOPS with pH 7.4

relatively broad range of NHS/EDC concentrations (for 0.9–6 mM).

Effect of concentration of NaCl in immobilization buffer

SSR varied very little for NaCl concentrations up to 10 mM NaCl after which it dropped significantly (see Fig. 4). We believe that this decrease was associated with interference of NaCl with the coupling efficiency of Ab to carboxylic groups leading to a decrease of the Ab density on AuNPs. The NaCl interfering effect was also observed for Ab immobilized on a flat surface of a SPR chip in control experiments (see ESM) and reported by Lofas et al. [28]. For lower NaCl concentrations, NSR also varied only slightly. The increase observed for higher NaCl concentrations was probably caused by a reduced Ab density on the surface of AuNPs. As SSR varied with NaCl concentration more than NSR (especially for high NaCl concentrations), *R* followed basically the same trend as SSR. Therefore, concentrations of NaCl close to zero provided the best conditions for the immobilization of Ab.

These results suggest that PBS (concentration of monovalent cations 140 mM) is not, despite its routine use [29–34], an appropriate immobilization buffer.

Effect of molarity of immobilization buffer

As depicted in Fig. 5, dependence of SSR, NSR, and *R* on buffer molarity followed the same trends as those observed when varying NaCl concentration (see previous section). This behavior was caused by the presence of sodium cations used to adjust the pH of the buffer (see ESM).

Effect of pH of immobilization buffer

As depicted in Fig. 6, both SSR and NSR depended on pH of the immobilization buffer only slightly and tended to decrease with increasing pH. This decrease may be attributed to a lower efficiency of the immobilization process (and thus lower amount of the attached Ab) or less favorable orientation of Ab at higher pH values. The latter effect was supported by our control experiments in which the specific sensor response

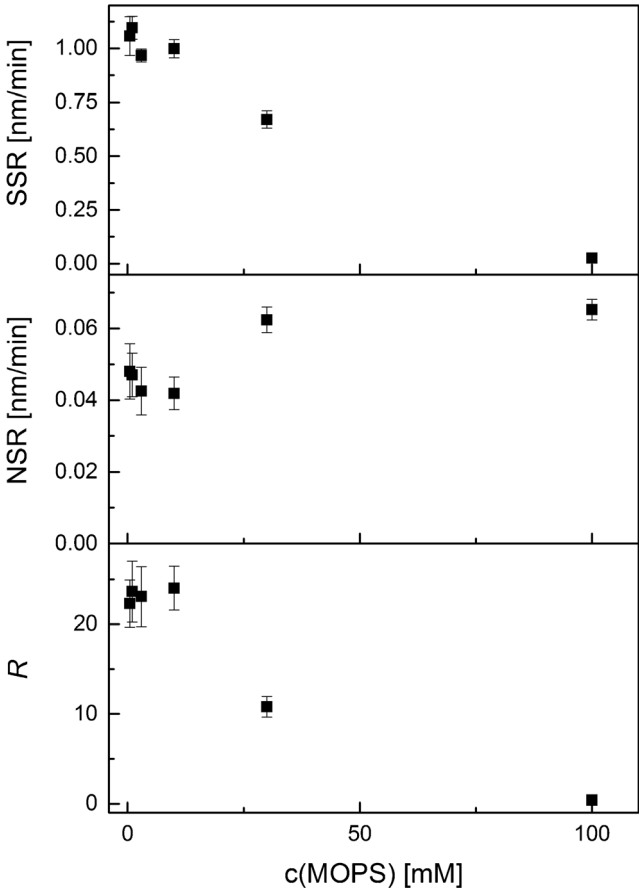

Fig. 5 SSR, NSR, and *R* for Ab-AuNPs prepared in immobilization buffers with different molarities. Preparation conditions kept constant: 3 mM NHS/EDC, 30 μg/mL Ab, 3 h reaction time, MOPS with 0 mM NaCl and pH 7.4

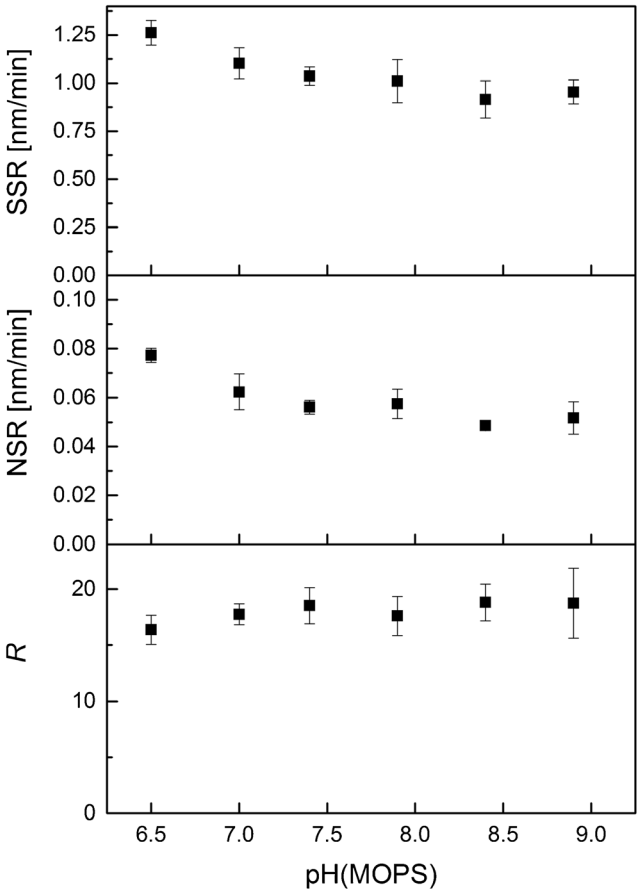

Fig. 6 SSR, NSR, and *R* for Ab-AuNPs prepared in different pH values of MOPS. Preparation conditions: 3 mM NHS/EDC, 30 μg/mL Ab, 3 h reaction time, 1 mM MOPS with 0 mM NaCl

to CEA was measured using Ab covalently attached to a flat surface of SPR chip under different pH values (see ESM); similar observations were also reported by other groups [35, 36]. Because of the weak dependencies of SSR and NSR on pH, *R* remained nearly constant across the whole pH range. This suggests that all the pH values within this range provide good immobilization conditions.

Effect of reaction time

As shown in Fig. 7, SSR increased with the reaction time up to about 3 h, when it leveled off. We think that this behavior was predominantly caused by the efficiency of immobilization (and thus the amount of immobilized Ab) which increased with the reaction time. Except for the shortest reaction time, NSR was increasing with the reaction time. Again, this trend was probably in a large part due to an increasing amount of Ab attached to the surface of an AuNP. *R* achieved the maximum at the reaction time of 3 h and did not vary much for the reaction times spanning from 1 to 6 h.

Binding properties of Ab-AuNPs

We prepared Ab-AuNPs under the optimum conditions (c(NHS/EDC) = 3 mM, c(Ab) = 30 μg/mL, T = 3 h, c(MOPS) = 1 mM, c(NaCl in MOPS) = 0 mM, pH (MOPS) = 7.4) and used them in the sandwich assay (see Fig. 1b) in order to characterize their binding to CEA molecules on the surface of the SPR chip (see Table 1 and Fig. 8).

In this work, we determined the binding efficiency of Ab-AuNPs to CEA, which describes the specific binding of Ab-AuNPs to CEA and has a direct impact on the Ab-AuNP-induced enhancement of SPR biosensor response [16]. We found that binding efficiencies as high as 63, 71, and 56% were achieved for CEA at concentrations of 62.5, 125, and 250 pg/mL in PBS_{BSA}, respectively (see Table 1). This suggests that AuNPs bound on average 63% of CEA molecules on the surface of a chip (assuming 1:1 interaction model).

To compare the binding efficiency of the developed Ab-AuNPs with the state of the art, we calculated binding efficiency of functional AuNPs reported in recent publications (see Table 1). Differences in sizes of the

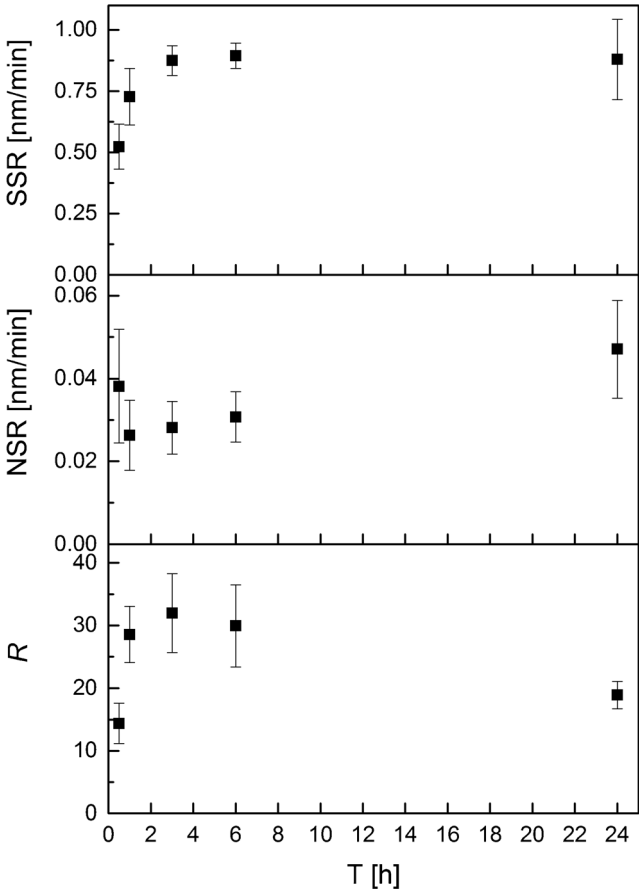

Fig. 7 SSR, NSR, and *R* for Ab-AuNPs prepared for the different reaction times of the activated AuNPs with Ab. Preparation conditions: 3 mM NHS/EDC, 30 μg/mL Ab, 1 mM MOPS with 0 mM NaCl and pH 7.4

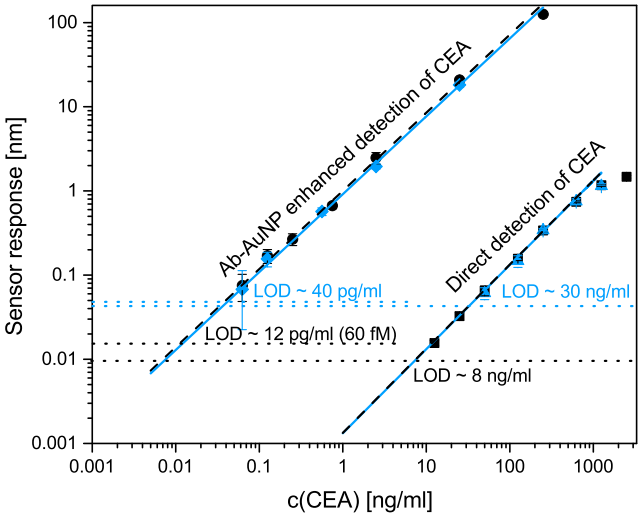

Fig. 8 Calibration curves for the direct and Ab-AuNP-enhanced detection of CEA in buffer (*black*) and 50% plasma (*blue*). The *error bars* denote the standard deviation of the sensor response for each concentration. The *dashed black lines* and *solid blue lines* show the linear fits; the *dotted lines* represent the sensor response corresponding to variation of the blank sample determined according to Student's *t* test. All the data are reference-compensated

used AuNPs were accounted for using the theory described in ref. [16]. Two approaches to the use of functional AuNPs in sandwich assays were described in the literature. In the first approach, antibody-coated AuNPs were captured in one step by analyte molecules, which were previously attached to the surface of a chip. In the second approach, streptavidin- or neutravidin-coated AuNPs were captured by biotinylated antibodies, which were previously bound to analyte molecules attached to the surface of a chip. We found the binding efficiencies of antibody-coated AuNPs to analytes to be from 1 to 15% and binding efficiencies of streptavidin- or neutravidin-coated AuNPs to biotinylated antibodies to be from 1 to 21%. The binding efficiencies were rather low in the published literature, which indicates low ability of functional AuNPs to bind to analyte on a surface.

Table 1 Performance of functionalized AuNPs in SPR biosensors

Type	Ref.	Chemistry	Analyte	Diameter of AuNP [nm]	Binding efficiency of AuNPs [%]	Enhancement of SPR signal	LOD [fM]
I.	This study	Ab, covalent	CEA	40	63	1000	60
	[8]	Ab, adsorbed	PSA	40	3.8	360	8500
	[8]	Ab, adsorbed	PSA	20	1.2	15	66,700
	[11]	Ab, adsorbed	PSA	23	15	115	35,100
	[13]	Ab, adsorbed	PSA	20	ND	ND	300
II.	[16]	N, covalent	CEA	52	3.4	56	ND
	[16]	N, covalent	CEA	33	13	50	ND
	[17]	S, covalent	CEA	30	21	180	500
	[14]	S, adsorbed	CEA	10	10	3	5000
	[12]	S, adsorbed	PSA	20	7.1	19	29,000
	[37]	S, ND	TNFα	20	1.2	3	211

Ab antibody, *N* neutravidin, *S* streptavidin, *ND* not determined

The Ab-AuNPs developed in this study provided binding efficiency that is more than 4 times better than the best functional AuNPs in the first group and 3 times better than the best functional AuNPs in the second group. It should be noted that this superior binding efficiency was obtained for rather big AuNPs (in comparison with the sizes of the functional AuNPs used in Table 1) in spite of the fact that big AuNPs suffer from steric effects that may reduce their binding efficiency [16]. It is also worth noting that AuNPs with covalently attached receptors exhibited in general higher binding efficiencies than AuNPs with adsorbed receptors (see Table 1). It might partly result from the fact that the covalently bound receptors are permanently attached to the surface of AuNPs and cannot be released from the AuNP surface during the binding of functional AuNPs to analyte molecules.

Ab-AuNP-based detection of CEA

We have investigated the performance of the optimized Ab-AuNPs in experiments in which we detected low concentrations of CEA in buffer and 50% plasma (see Table 1 and Fig. 8). The combination of the superior binding efficiency of Ab-AuNPs and the high pure optical enhancement of rather big AuNPs [16] allowed our Ab-AuNPs to enhance the response of an SPR biosensor to CEA by a factor of 1000 and 900 for CEA in PBS_{BSA} and 50% plasma, respectively. This enhancement significantly exceeded the enhancements reported in the literature (see Table 1). Because of the high enhancement of Ab-AuNPs and very low nonspecific binding of Ab-AuNPs (~1 Ab-AuNP per 50 μm^2 and 1 Ab-AuNP per 20 μm^2 for CEA in PBS_{BSA} and 50% plasma, respectively), we were able to achieve LODs as low as 12 pg/mL (60 fM) in buffer and 40 pg/mL (200 fM) in 50% plasma. The demonstrated LODs are currently the best LODs achieved for AuNP-enhanced SPR biosensor-based detection of CEA [14, 17]. Moreover, the LOD in buffer (60 fM) is comparable with or better than the LODs achieved recently for CEA in buffer by electrochemical [38–42], chemiluminescence [43, 44], inductively coupled plasma mass spectrometric [45], and surface acoustic wave [46] biosensors that typically range from 5 to 5000 fM (see also Table S5 in ESM).

Conclusions

In this work, we investigated the effect of preparation conditions on the performance of functional AuNPs in optical affinity biosensors. We found that preparation conditions, such as concentration of antibody, concentration of NHS/EDC activation reagents, composition of immobilization buffer (molarity, salt content), and reaction time, have potentially significant effect on the performance of antibody-coated AuNPs. Our study suggests that the optimum conditions for the functionalization of AuNPs with antibodies include concentration of antibody in microgram per milliliter range, concentration of NHS/EDC reagents in millimolar range, concentration of NaCl up to 3 mM, buffer molarity up to 10 mM (for MOPS), and reaction time in the order of hours.

We further prepared AuNPs functionalized with antibody against CEA under the optimum conditions and demonstrated that these Ab-AuNPs offer binding efficiency as high as 63% which presents more than fourfold improvement when compared with the best results obtained for antibody-coated AuNPs so far. Moreover, we demonstrated that Ab-AuNPs prepared under the optimum conditions were able to enhance SPR sensor response by three orders of magnitude and to detect CEA at concentrations as low as 12 pg/mL (60 fM) in buffer and 40 pg/mL (200 fM) in 50% blood plasma, which is currently the most sensitive AuNP-enhanced SPR biosensor-based detection of CEA. This illustrates the importance of careful functionalization of AuNPs and the vast potential of functional AuNPs for ultrasensitive optical biosensors in a variety of fields, such as medical diagnostics, environmental monitoring, food safety, and security.

Acknowledgements This research was supported by the Czech Science Foundation (contract no. GBP205/12/G118) and by Praemium Academiae of the Czech Academy of Sciences.

Compliance with ethical standards

Conflict of interest The authors declare that they have no conflicts of interest.

References

1. Cao X, Ye Y, Liu S. Gold nanoparticle-based signal amplification for biosensing. Anal Biochem. 2011;417(1):1–16.
2. Tothill IE. Biosensors for cancer markers diagnosis. Semin Cell Dev Biol. 2009;20(1):55–62.
3. Špačková B, Wrobel P, Bocková M, Homola J. Optical biosensors based on plasmonic nanostructures: a review. Proc IEEE. 2016;104(12):2380–408.
4. Stoeva SI, Lee JS, Thaxton CS, Mirkin CA. Multiplexed DNA detection with biobarcoded nanoparticle probes. Angew Chem Int Edit. 2006;45(20):3303–6.
5. Golub E, Pelossof G, Freeman R, Zhang H, Willner I. Electrochemical, photoelectrochemical, and surface plasmon resonance detection of cocaine using supramolecular aptamer complexes and metallic or semiconductor nanoparticles. Anal Chem. 2009;81(22):9291–8.
6. Zahavy E, Whitesell JK, Fox MA. Surface effects in water-soluble shell-core hybrid gold nanoparticles in oligonucleotide single strand recognition for sequence-specific bioactivation. Langmuir. 2010;26(21):16442–6.
7. Stoeva SI, Lee JS, Smith JE, Rosen ST, Mirkin CA. Multiplexed detection of protein cancer markers with biobarcoded nanoparticle probes. J Am Chem Soc. 2006;128(26):8378–9.

8. Uludag Y, Tothill IE. Cancer biomarker detection in serum samples using surface plasmon resonance and quartz crystal microbalance sensors with nanoparticle signal amplification. Anal Chem. 2012;84(14):5898–904.
9. Sapsford KE, Algar WR, Berti L, Gemmill KB, Casey BJ, Oh E, Stewart MH, Medintz IL. Functionalizing nanoparticles with biological molecules: developing chemistries that facilitate nanotechnology. Chem Rev. 2013;113(3):1904–2074.
10. Sperling RA, Parak WJ. Surface modification, functionalization and bioconjugation of colloidal inorganic nanoparticles. Philos Trans A Math Phys Eng Sci. 2010;368(1915):1333–83.
11. Cao C, Sim SJ. Double-enhancement strategy: a practical approach to a femto-molar level detection of prostate specific antigen-alpha(1)-antichymotrypsin (PSA/ACT complex) for SPR immunosensing. J Microbiol Biotechnol. 2007;17(6):1031–5.
12. Huang L, Reekmans G, Saerens D, Friedt JM, Frederix F, Francis L, Muyldermans S, Campitelli A, Van Hoof C. Prostate-specific antigen immunosensing based on mixed self-assembled monolayers, camel antibodies and colloidal gold enhanced sandwich assays. Biosens Bioelectron. 2005;21(3):483–90.
13. Cho JW, Kang DY, Jang YH, Kim HH, Min J, Oh BK. Ultrasensitive surface plasmon resonance based immunosensor for prostate-specific antigen using gold nanoparticle-antibody complex. Colloid Surface A. 2008;313:655–9.
14. Li R, Feng F, Chen ZZ, Bai YF, Guo FF, Wu FY, Zhou G. Sensitive detection of carcinoembryonic antigen using surface plasmon resonance biosensor with gold nanoparticles signal amplification. Talanta. 2015;140:143–9.
15. Uludag Y, Tothill IE. Development of a sensitive detection method of cancer biomarkers in human serum (75%) using a quartz crystal microbalance sensor and nanoparticles amplification system. Talanta. 2010;82(1):277–82.
16. Špringer T, Ermini ML, Špačková B, Jablonků J, Homola J. Enhancing sensitivity of surface plasmon resonance biosensors by functionalized gold nanoparticles: size matters. Anal Chem. 2014;86(20):10350–6.
17. Špringer T, Homola J. Biofunctionalized gold nanoparticles for SPR-biosensor-based detection of CEA in blood plasma. Anal Bioanal Chem. 2012;404(10):2869–75.
18. Bartczak D, Kanaras AG. Preparation of peptide-functionalized gold nanoparticles using one pot EDC/sulfo-NHS coupling. Langmuir. 2011;27(16):10119–23.
19. Bastus NG, Comenge J, Puntes V. Kinetically controlled seeded growth synthesis of citrate-stabilized gold nanoparticles of up to 200 nm: size focusing versus Ostwald ripening. Langmuir. 2011;27(17):11098–105.
20. Haiss W, Thanh NT, Aveyard J, Fernig DG. Determination of size and concentration of gold nanoparticles from UV-vis spectra. Anal Chem. 2007;79(11):4215–21.
21. Vaisocherová H, Zítová A, Lachmanová M, Štěpánek J, Králíková S, Liboška R, Rejman D, Rosenberg I, Homola J. Investigating oligonucleotide hybridization at subnanomolar level by surface plasmon resonance biosensor method. Biopolymers. 2006;82(4):394–8.
22. Špringer T, Piliarik M, Homola J. Surface plasmon resonance sensor with dispersionless microfluidics for direct detection of nucleic acids at the low femtomole level. Sensor Actuat B-Chem. 2010;145(1):588–91.
23. Špringer T, Piliarik M, Homola J. Real-time monitoring of biomolecular interactions in blood plasma using a surface plasmon resonance biosensor. Anal Bioanal Chem. 2010;398(5):1955–61.
24. Špringer T, Bocková M, Homola J. Label-free biosensing in complex media: a referencing approach. Anal Chem. 2013;85(12):5637–40.
25. Saha B, Evers TH, Prins MWJ. How antibody surface coverage on nanoparticles determines the activity and kinetics of antigen capturing for biosensing. Anal Chem. 2014;86(16):8158–66.
26. Silin V, Weetall H, Vanderah DJ. SPR studies of the nonspecific adsorption kinetics of human IgG and BSA on gold surfaces modified by self-assembled monolayers (SAMs). J Colloid Interf Sci. 1997;185(1):94–103.
27. Jones S, Thornton JM. Principles of protein-protein interactions. Proc Natl Acad Sci U S A. 1996;93(1):13–20.
28. Johnsson B, Lofas S, Lindquist G. Immobilization of proteins to a carboxymethyldextran-modified gold surface for biospecific interaction analysis in surface-plasmon resonance sensors. Anal Biochem. 1991;198(2):268–77.
29. Eck W, Craig G, Sigdel A, Ritter G, Old LJ, Tang L, Brennan MF, Allen PJ, Mason MD. PEGylated gold nanoparticles conjugated to monoclonal F19 antibodies as targeted labeling agents for human pancreatic carcinoma tissue. ACS Nano. 2008;2(11):2263–72.
30. Gao J, Huang X, Liu H, Zan F, Ren J. Colloidal stability of gold nanoparticles modified with thiol compounds: bioconjugation and application in cancer cell imaging. Langmuir. 2012;28(9):4464–71.
31. Di Pasqua AJ, Mishler RE, Ship YL, Dabrowiak JC, Asefa T. Preparation of antibody-conjugated gold nanoparticles. Mater Lett. 2009;63(21):1876–9.
32. Eck W, Nicholson AI, Zentgraf H, Semmler W, Bartling S. Anti-CD4-targeted gold nanoparticles induce specific contrast enhancement of peripheral lymph nodes in X-ray computed tomography of live mice. Nano Lett. 2010;10(7):2318–22.
33. Huang T, Nallathamby PD, Gillet D, Xu XH. Design and synthesis of single-nanoparticle optical biosensors for imaging and characterization of single receptor molecules on single living cells. Anal Chem. 2007;79(20):7708–18.
34. Liu T, Thierry B. A solution to the PEG dilemma: efficient bioconjugation of large gold nanoparticles for biodiagnostic applications using mixed layers. Langmuir. 2012;28(44):15634–42.
35. Pei ZC, Anderson H, Myrskog A, Duner G, Ingemarsson B, Aastrup T. Optimizing immobilization on two-dimensional carboxyl surface: pH dependence of antibody orientation and antigen binding capacity. Anal Biochem. 2010;398(2):161–8.
36. Puertas S, Batalla P, Moros M, Polo E, Del Pino P, Guisan JM, Grazu V, de la Fuente JM. Taking advantage of unspecific interactions to produce highly active magnetic nanoparticle-antibody conjugates. ACS Nano. 2011;5(6):4521–8.
37. Martinez-Perdiguero J, Retolaza A, Bujanda L, Merino S. Surface plasmon resonance immunoassay for the detection of the TNF alpha biomarker in human serum. Talanta. 2014;119:492–7.
38. Wu W, Yi P, He P, Jing T, Liao KL, Yang K, Wang HD. Nanosilver-doped DNA polyion complex membrane for electrochemical immunoassay of carcinoembryonic antigen using nanogold-labeled secondary antibodies. Anal Chim Acta. 2010;673(2):126–32.
39. Zhong ZY, Wu W, Wang D, Wang D, Shan JL, Qing Y, Zhang ZM. Nanogold-enwrapped graphene nanocomposites as trace labels for sensitivity enhancement of electrochemical immunosensors in clinical immunoassays: carcinoembryonic antigen as a model. Biosens Bioelectron. 2010;25(10):2379–83.
40. Song ZJ, Yuan R, Chai YQ, Jiang W, Su HL, Che X, Ran XQ. Simultaneous immobilization of glucose oxidase on the surface and cavity of hollow gold nanospheres as labels for highly sensitive electrochemical immunoassay of tumor marker. Biosens Bioelectron. 2011;26(5):2776–80.
41. Tang J, Tang DP, Li QF, Su BL, Qiu B, Chen GN. Sensitive electrochemical immunoassay of carcinoembryonic antigen with signal dual-amplification using glucose oxidase and an artificial catalase. Anal Chim Acta. 2011;697(1–2):16–22.
42. Zhang YY, Xiang Y, Chai YQ, Yuan R, Qian XQ, Zhang HX, Chen Y, Su J, Xu J. Gold nanolabels and enzymatic recycling dual amplification-based electrochemical immunosensor for the highly

sensitive detection of carcinoembryonic antigen. Sci China Chem. 2011;54(11):1770–6.
43. Hao MJ, Ma ZF. An ultrasensitive chemiluminescence biosensor for carcinoembryonic antigen based on autocatalytic enlargement of immunogold nanoprobes. Sensors. 2012;12(12):17320–9.
44. Chen LL, Zhang ZJ, Zhang P, Zhang XM, Fu AH. An ultrasensitive chemiluminescence immunosensor of carcinoembryonic antigen using HRP-functionalized mesoporous silica nanoparticles as labels. Sensor Actuat B-Chem. 2011;155(2):557–61.
45. Liu R, Liu X, Tang YR, Wu L, Hou XD, Lv Y. Highly sensitive immunoassay based on Immunogold-silver amplification and inductively coupled plasma mass spectrometric detection. Anal Chem. 2011;83(6):2330–6.
46. Zhang X, Zou YC, An C, Ying KJ, Chen X, Wang P. Sensitive detection of carcinoembryonic antigen in exhaled breath condensate using surface acoustic wave immunosensor. Sensor Actuat B-Chem. 2015;217:100–6.